



Cite this: *Chem. Sci.*, 2020, **11**, 11843

All publication charges for this article have been paid for by the Royal Society of Chemistry

Received 5th August 2020

Accepted 6th October 2020

DOI: 10.1039/d0sc04285d

rsc.li/chemical-science

Introduction

Photocatalysts are promising materials for the conversion of solar energy into storable chemical energy and are expected to contribute significantly to clean and renewable energy generation.¹ In 1974, Fujishima and Honda reported photocatalytic water-splitting using a titanium dioxide electrode, demonstrating the possibility of artificial photosynthesis.² Since then, a wide range of photocatalysts, based on inorganic,³ molecular,⁴ and polymeric⁵ compounds, have been actively developed. Besides their application in artificial photosynthesis, the redox reactivity of photocatalysts has been utilized for environmental remediation,⁶ organic synthesis,⁷ and photodynamic therapy.⁸ The emergence and development of new photocatalysts have contributed to the progress in artificial photosynthesis and generated new opportunities in the related fields.⁹

Based on these backgrounds, we explored a new class of photocatalysts and focused on supramolecular assemblies. The

photophysical properties of supramolecular assemblies are different from those of the constituting monomers because of the interaction between the adjacent molecules.¹⁰ Various characteristic aggregation-induced photophysical phenomena, such as aggregation-caused quenching (ACQ),¹¹ aggregation-induced enhanced emission,¹² light-harvesting,¹³ and nonlinear optical phenomena (e.g., photon upconversion¹⁴ and singlet fission¹⁵) have been intensively studied and applied to solar energy collection,¹⁶ molecular sensing,¹⁷ and biological applications (e.g., bioimaging,¹⁸ optogenetics,¹⁹ and phototherapy²⁰). However, aggregation-induced photocatalytic activity (AI-PCA) has never been reported despite the high potential for a novel photocatalytic material. Taking into account previous reports on aggregation-induced triplet excited state generation²¹ and charge carrier migration²² in self-assembled nanostructures of organic dyes, we considered that various organic dyes may cause AI-PCA. These phenomena cause elongation of the excited state lifetime²³ and increasing collision frequency with substrates,²⁴ which are important for the progression of photocatalytic reactions. AI-PCA would lead to expansion of the molecular design of photocatalysts that enables adjustment of absorption wavelength and redox potential. In addition, self-assembled supramolecular photocatalysts (SA-SPCs) possessing AI-PCA are expected to produce unprecedented photocatalytic soft-materials²⁵ (gel, liquid crystal, membrane *etc.*) taking advantages of the unique properties of supramolecular assemblies²⁶ (e.g. reversibility and stimuli-responsiveness).

Herein, we demonstrate the AI-PCA of amphiphilic rhodamines (Fig. 1a). Rhodamines are very common hydrophilic organic dyes with excellent photophysical properties, such as high light absorption and quantum yield, which can be tuned

^aDepartment of Applied Chemistry, Graduate School of Engineering, Osaka University, Suita 565-0871, Japan. E-mail: shigemitsu@chem.eng.osaka-u.ac.jp; kida@chem.eng.osaka-u.ac.jp

^bFrontier Research Base for Global Young Researchers, Graduate School of Engineering, Osaka University, Suita 565-0871, Japan

^cGlobal Center for Medical Engineering and Informatics, Osaka University, Suita 565-0871, Japan

^dThe Institute of Scientific and Industrial Research (SANKEN), Osaka University, Mihogaoka 8-1, Ibaraki, Osaka 567-0047, Japan

^eInstitute for Advanced Co-creation Studies, Osaka University, 1-1 Yamadagaoka, Suita, Osaka, 565-0871, Japan

† Electronic supplementary information (ESI) available. See DOI: [10.1039/d0sc04285d](https://doi.org/10.1039/d0sc04285d)



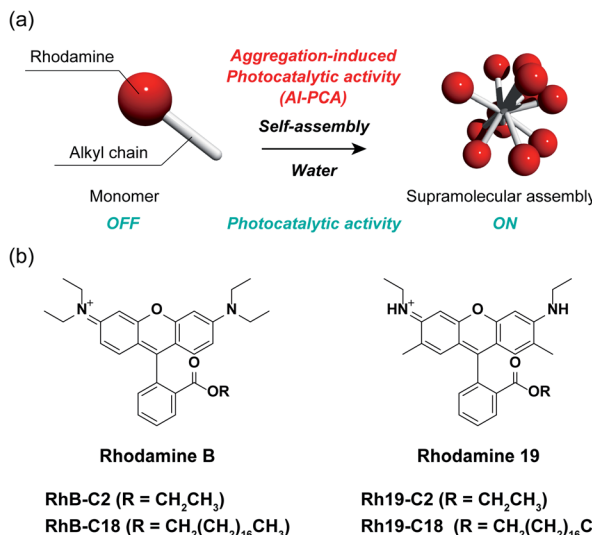


Fig. 1 (a) Schematic representation of aggregation-induced photocatalytic activity (AI-PCA). (b) Chemical structures of rhodamine derivatives (left: rhodamine B (RhB), and right: rhodamine 19 (Rh19)).

through chemical modification.²⁷ The two SA-SPCs composed of amphiphilic rhodamines (rhodamine B (**RhB**) and rhodamine 19 (**Rh19**) (Fig. 1b)) exhibited photocatalytic activity under visible light irradiation in water, while the monomeric rhodamines did not exhibit photocatalytic activity. In particular, the SA-SPCs exhibited excellent hydrogen evolution rates.

Results and discussion

Molecular design of the rhodamine derivatives

Four rhodamine derivatives with short and long alkyl chains were used in this study (Fig. 1b). Two common rhodamines with different absorption bands, **RhB** and **Rh19**, were selected as hydrophilic organic dyes to examine the concept of AI-PCA. The amphiphilic rhodamines with octadecyl alkyl chains (**RhB-C18** and **Rh19-C18**) were expected to form supramolecular assemblies in water through hydrophobic interaction between the alkyl chains. More hydrophilic rhodamine derivatives with an ethyl ester group (**RhB-C2** and **Rh19-C2**) compared to those with octadecyl alkyl chains were prepared as control compounds to evaluate the effect of self-assembly on the photocatalytic activity.

The photophysical properties of monomeric **RhB-C2** and **RhB-C18** were evaluated from their UV-vis absorption (UV-vis) and photoluminescence (PL) spectra measured in dimethyl sulfoxide (DMSO), which is a good solvent for these compounds (Fig. 2a and b). The absorption spectra of **RhB-C2** and **RhB-C18** corresponded well with each other (Fig. 2a) and both the compounds exhibited absorption maxima at 566 nm. **RhB-C2** and **RhB-C18** also exhibited similar PL spectra with an emission peak at $\lambda_{\text{em}} = 592$ nm (Fig. 2b). These results indicate that the electronic states of **RhB-C2** and **RhB-C18** are quite similar despite the different alkyl chain lengths. We thus conclude that this pair is suitable for evaluating the effect of self-assembly on their photophysical and photocatalytic properties. Further,

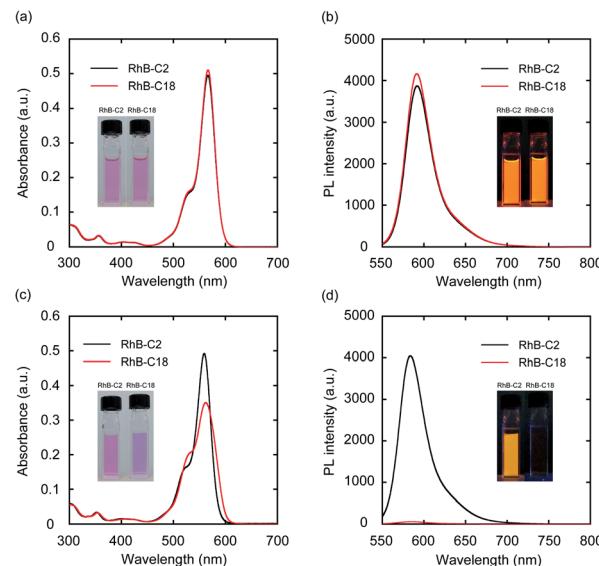


Fig. 2 (a, c) UV-vis absorption (UV-vis) and (b, d) photoluminescence (PL) spectra of **RhB-C2** and **RhB-C18** in DMSO (a, b) and water (c, d). Experimental conditions: $[\text{RhB-C2}] = [\text{RhB-C18}] = 5.0 \mu\text{M}$, rt, water, excitation wavelength: 540 nm. Insets: Optical photos of **RhB-C2** and **RhB-C18** in DMSO and water under (a, c) daylight and (b, d) UV light (365 nm).

Rh19-C2 and **Rh19-C18** also exhibited similar UV-vis and PL spectra (Fig. S1a and b[†]) with maxima at $\lambda_{\text{abs}} = 539$ nm and $\lambda_{\text{em}} = 565$ nm, respectively, which indicate that the **Rh19-C2/Rh19-C18** pair has similar electronic states regardless of the alkyl chain length.

Self-assembling properties of the rhodamines in water

To examine the self-assembly properties, the UV-vis and PL spectra of **RhB-C2** and **RhB-C18** were recorded in water (concentration: $5.0 \mu\text{M}$) (Fig. 2c and d). The UV-vis spectrum of **RhB-C2** in water is similar to that in DMSO with a slightly red-shifted absorption maximum ($\lambda_{\text{abs}} = 559$ nm (DMSO), 562 nm (water)) (Fig. 2c). In contrast, **RhB-C18** exhibited a broad spectrum with split peaks at 530 and 559 nm that can be assigned to the aggregation states of **RhB-C18**,²⁸ which suggests the formation of a supramolecular assembly of **RhB-C18** in water. The PL spectra of **RhB-C2** and **RhB-C18** were significantly different (Fig. 2d). **RhB-C2** exhibited an intense emission in water, whereas **RhB-C18** exhibited a very weak emission. This suggests ACQ in **RhB-C18**.¹¹ Furthermore, the addition of a nonionic surfactant (Triton X-100, 0.3 vol%) to the **RhB-C18** aqueous solution drastically increased the PL intensity (Fig. S2b[†]), which suggests the dissociation of the **RhB-C18** supramolecular assembly by Triton X-100. The photophysical properties of the **Rh19-C2/Rh19-C18** pair exhibited the same trend as those of the **RhB-C2/RhB-C18** pair (Fig. S1c, d and S2c, d[†]). **Rh19-C18** formed supramolecular assemblies, whereas **Rh19-C2** did not form supramolecular assemblies in water. With the increasing concentration, the absorbances of the rhodamine derivatives measured in water increased linearly (Fig. S3 and S4[†]); this indicates that **RhB-C2** and **Rh19-C2** did



not form supramolecular assemblies until 50 μM (Fig. S3 \dagger), and the excessive aggregation of **RhB-C18** and **Rh19-C18** did not occur at least until 100 μM (Fig. S4 \dagger).

Dynamic light scattering (DLS) measurements and transmission electron microscopy (TEM) observations were performed to confirm the formation of supramolecular assemblies. DLS measurements indicated the presence of supramolecular assemblies of **RhB-C18** and **Rh19-C18** having average sizes of 200 and 82 nm, respectively (Fig. S5a and b \dagger). TEM revealed the formation of spherical supramolecular assemblies of **RhB-C18** and **Rh19-C18** (Fig. S5c and d \dagger). The selected area electron diffraction (SAED) patterns obtained by TEM exhibited diffused rings and no diffraction spots, which indicate the amorphous nature of the rhodamine supramolecular assemblies (Fig. S5e and f \dagger).

Photocatalytic activities of the rhodamines in water

Since it became clear that the rhodamine pairs were suitable for evaluation of AI-PCA, we initially examined their photocatalytic activities in water using 1,1',3,3,3',3'-hexamethylindotricarbocyanine iodide (**HITCI**) (Fig. S6a \dagger).²⁹ The rhodamines and **HITCI** were mixed in water, and the UV-vis spectra were recorded after photoirradiation of the mixture ($\lambda = 560$ nm (FWHM: 10 nm, Xe lamp, 300 W)). In the case of **RhB-C2**, the absorption band at around 735 nm arising from **HITCI** gradually decreased (Fig. 3a). Considering the self-photooxidation of **HITCI** upon photoirradiation (Fig. S6b and c \dagger), the photocatalytic activity of **RhB-C2** in **HITCI** oxidation is considered

negligible. In contrast, **RhB-C18** remarkably oxidized **HITCI** within a short period of photoirradiation (Fig. 3b and c). In addition, similar to **RhB-C2**, **Rh19-C2** caused slow degradation of **HITCI** (Fig. S7a \dagger), whereas the supramolecular assemblies of **Rh19-C18** rapidly degraded **HITCI** (Fig. S7b and c \dagger). The rate of **HITCI** oxidation by the rhodamines was estimated to be 8.2×10^{-3} , 3.1×10^{-1} , 2.9×10^{-3} , and 1.0×10^{-1} min^{-1} for **RhB-C2**, **RhB-C18**, **Rh19-C2**, and **Rh19-C18**, respectively, by linear regression fitting (Fig. 3d and S7d \dagger). Compared with **RhB-C2** and **Rh19-C2**, **RhB-C18** and **Rh19-C18** accelerated **HITCI** oxidation 39-fold and 34-fold, respectively. Additionally, in the presence of Triton X-100, the rates of **HITCI** photooxidation by the **RhB-C2/RhB-C18** and **Rh19-C2/Rh19-C18** pairs were almost the same (Fig. S8 \dagger). These results indicate that the formation of supramolecular assemblies of rhodamines enhanced the oxidation of **HITCI**.

Mechanistic study on the photocatalytic activity of the rhodamine SA-SPCs

The photoreaction of SA-SPCs is considered to occur *via* two types of mechanisms involving electron and/or energy transfer processes.³⁰ Under aerobic conditions, in the energy transfer process, singlet oxygen (${}^1\text{O}_2$) is commonly involved in the photocatalytic reaction, whereas oxygen radicals such as superoxide anion radicals ($\text{O}_2^{\cdot-}$) and hydroxyl radicals ($\text{OH}^{\cdot-}$) are involved in the electron transfer mechanism (Fig. S9 \dagger).³¹ To explain the mechanism of the photocatalytic reaction, electron spin resonance (ESR) spectroscopy was performed using 4-hydroxy-2,2,6,6-tetramethylpiperidine (4-OH-TEMP)³² and 5,5-dimethyl-1-pyrroline *N*-oxide (DMPO)³³ as spin trap reagents to detect ${}^1\text{O}_2$ and oxygen radicals (*e.g.* $\text{O}_2^{\cdot-}$, $\text{OH}^{\cdot-}$), respectively (Fig. S10a and b \dagger). The ESR experimental conditions were first determined using Rose Bengal (Fig. S10c \dagger) as a standard.³⁴ The ESR spectra of **RhB-C2** and **RhB-C18** exhibited a characteristic 1 : 1 : 1 triplet corresponding to the TEMPOL radical (Fig. 4a). **RhB** generates a triplet state despite the low quantum yield of intersystem crossing (quantum yield (Φ_T): 0.006).³⁵ Therefore, it is reasonable that **RhB-C2** exhibited an ESR signal for the TEMPOL radical. No significant differences were observed in the signal intensities of the TEMPOL radicals of **RhB-C2** and **RhB-C18**, which implies that the rate of energy transfer to oxygen did not drastically change after self-assembly. These results suggest that the photocatalytic reaction of **RhB-C18** does not occur through the energy transfer mechanism. Subsequently, we evaluated the generation of oxygen radical species *via* the electron transfer mechanism. The ESR spectrum for **RhB-C2** in DMPO did not exhibit a clear signal for a DMPO adduct (Fig. 4b), whereas the ESR spectrum of **RhB-C18** exhibited a signal for a DMPO hydroxyl radical adduct (DMPO-OH). Since the superoxide anion ($\text{O}_2^{\cdot-}$) is unstable in aqueous media, it reacts with protons immediately upon addition to an aqueous medium (Fig. S9a \dagger) and does not react with DMPO to form DMPO-OOH. Hence, no DMPO-OOH peak appeared in the ESR spectrum. However, we confirmed the generation of a hydroxyl radical ($\text{OH}^{\cdot-}$) that was produced by the chain reaction starting from $\text{O}_2^{\cdot-}$ ions through electron transfer in water (Fig. 4b, c and

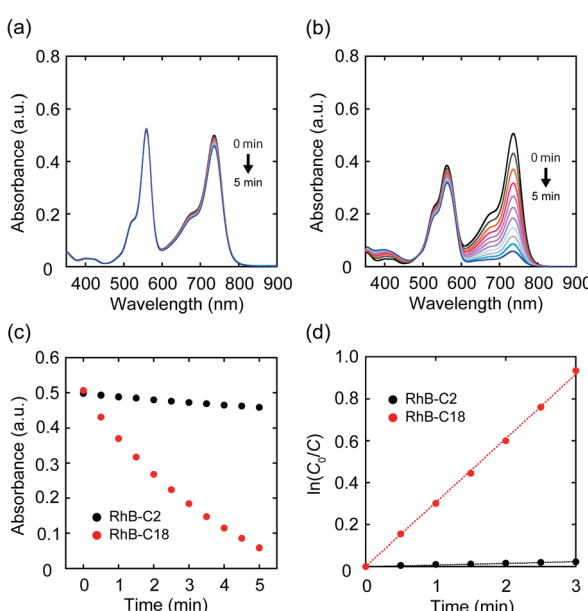


Fig. 3 (a, b) UV-vis absorption spectra of the mixture of **HITCI** with (a) **RhB-C2** and (b) **RhB-C18** after photoirradiation. (c) Time-course of absorbance at 735 nm after photoirradiation using **RhB-C2** (black circle) and **RhB-C18** (red circle). (d) Linear regression plots of **HITCI** absorbance with **RhB-C2** (black circle) and **RhB-C18** (red circle). Experimental conditions: $[\text{RhB-C2}] = [\text{RhB-C18}] = 5.0 \mu\text{M}$, $[\text{HITCI}] = 2.5 \mu\text{M}$ solvent: water, rt, irradiation wavelength: 560 nm (FWHM: 10 nm, Xe lamp, 300 W).



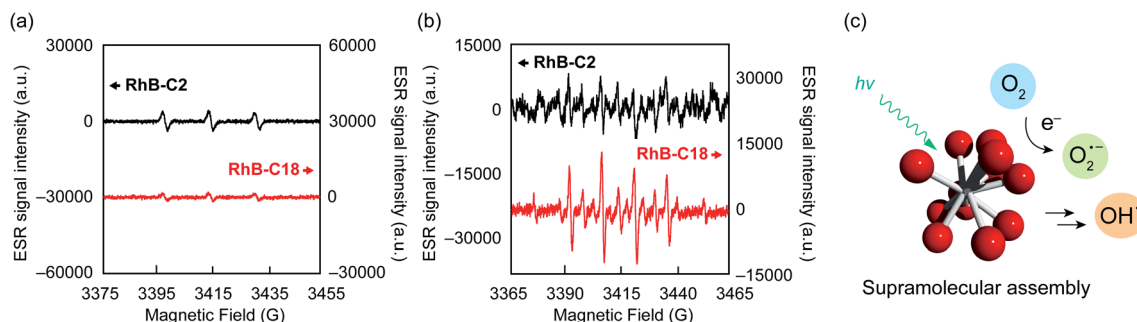


Fig. 4 ESR signals of (a) 4-OH-TEMP and (b) DMPO adducts observed for **RhB-C2** and **RhB-C18** after light irradiation. (c) Schematic representation of generation of a hydroxyl radical through electron transfer and chain reactions. Experimental conditions: $[\text{RhB-C2}] = [\text{RhB-C18}] = 50 \mu\text{M}$, $[4\text{-OH-TEMP}] = [\text{DMPO}] = 100 \text{ mM}$, solvent: water, rt, irradiation wavelength: 560 nm (FWHM: 10 nm, Xe lamp, 300 W, 3 min).

S9a†). The experimental results showed that **RhB-C18** exhibits photocatalytic activity mainly through an electron transfer mechanism. Further, the ESR spectra of the **Rh19-C2/Rh19-C18** pair were similar to those of the **RhB-C2/RhB-C18** pair (Fig. S11†).

Photocatalytic hydrogen evolution using the rhodamine SA-SPCs

Photocatalytic hydrogen evolution is one of the important reactions toward realizing artificial photosynthesis.² The hydrogen evolution abilities of various photocatalysts have been actively examined to date. The electron transfer mechanism of the SA-SPC encouraged us to investigate the photocatalytic hydrogen evolution by the rhodamine SA-SPCs using Pt nanoparticles as a co-catalyst and ascorbic acid (Asc) as a sacrificial reagent (Fig. 5a). The HOMO levels of the rhodamine derivatives (Table S1,† **RhB-C2**: -5.4 eV , **RhB-C18**: -5.5 eV **Rh19-C2**: -5.4 eV , and **Rh19-C18**: -5.5 eV) determined by cyclic voltammetry or square wave voltammetry (Fig. S12 and S13†) were sufficiently lower than that of Asc (-4.6 eV),³⁶ while the LUMO levels of the rhodamine derivatives (Table S1,† **RhB-C2**: -3.2 eV , **RhB-C18**: -3.5 eV **Rh19-C2**: -3.1 eV , and **Rh19-C18**: -3.4 eV) were enough for the proton reduction reaction. The addition of Asc and H_2PtCl_6 as a precursor of Pt nanoparticles hardly affected the size of SA-SPCs (Fig. S14a and b†).

The time-courses of photocatalytic hydrogen evolution by **RhB-C2** and **RhB-C18** are shown in Fig. 5b. After light irradiation ($\lambda > 360 \text{ nm}$, 300 W (Xe lamp)), Pt nanoparticles were formed (Fig. S14c-f†) and **RhB-C18** exhibited hydrogen generation, while **RhB-C2** did not display hydrogen evolution. The **RhB-C18** SA-SPC functioned for 80 min without any decrease in the photocatalytic activity, and the average hydrogen evolution rate (HER) was determined to be $3.7 \text{ mmol g}^{-1} \text{ h}^{-1}$ (Fig. 5b), which is comparable to that of other excellent organic systems such as $\text{g-C}_3\text{N}_4$ ($0.67 \text{ mmol g}^{-1} \text{ h}^{-1}$)³⁷ and a covalent organic framework ($10.1 \text{ mmol g}^{-1} \text{ h}^{-1}$).³⁸ 80 min after light irradiation, the photocatalytic activities of the SA-SPCs decreased due to the decomposition of rhodamines. **Rh19-C18** exhibited photocatalytic hydrogen evolution (HER: $2.9 \text{ mmol g}^{-1} \text{ h}^{-1}$), while **Rh19-C2** did not (Fig. S15a†). One of the reasons for the high HER would be intermolecular electron migration among the rhodamines.³⁹ The photoirradiation of rhodamines generated intermolecular charge separation states, and the migration between the rhodamines may have facilitated efficient electron transfer to the Pt nanoparticle. The apparent quantum efficiencies of **RhB-C18** and **Rh19-C18** were 0.059 and 0.039% under these conditions, respectively.

To examine the effects of the SA-SPC concentration on the hydrogen evolution reaction, the SA-SPC concentrations were increased from 50 to 100 μM . The amorphous self-assembled spherical structures were almost unchanged (Fig. S16,† average particle diameter: **RhB-C18**: 223 nm, **Rh19-C18**: 122 nm) after the increase. The hydrogen evolution rates decreased from 3.7 to $2.4 \text{ mmol g}^{-1} \text{ h}^{-1}$ for **RhB-C18** (Fig. S17a†). On the other hand, in the case of **Rh19-C18**, the hydrogen evolution rate significantly increased from 2.9 to $5.9 \text{ mmol g}^{-1} \text{ h}^{-1}$ (Fig. S17b†). These results indicate that the hydrogen evolution rates are significantly affected by the concentration of the SA-SPC. The versatile factors including the size, morphology, surface area, fluidity, and electric state of the SA-SPC, and interactions between the SA-SPC and Pt nanoparticles or ascorbic acid would have a sensitive effect on the hydrogen evolution. A detailed understanding of the changes of **RhB-C18** and **Rh19-C18** for photocatalytic hydrogen evolution rates is currently difficult. We will study how each factor has effects on photocatalytic activity in future studies.

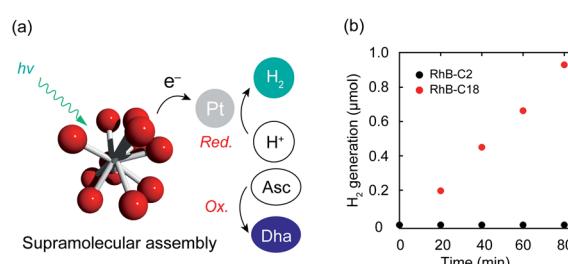


Fig. 5 (a) Schematic representation of photocatalytic hydrogen evolution by the SA-SPC composed of rhodamine derivatives. (b) Time-course of hydrogen evolution by **RhB-C18** and **RhB-C18** under visible light. Experimental conditions: $[\text{rhodamines}] = 50 \mu\text{M}$, $[\text{Pt}] = 100 \mu\text{M}$, $[\text{Asc}] = 500 \text{ mM}$, solvent: water, rt, irradiation light wavelength: $>360 \text{ nm}$. Asc: ascorbic acid, DHA: dehydroascorbic acid.



Conclusions

In summary, we demonstrated the AI-PCA of two rhodamine derivatives. The rhodamine SA-SPCs showed excellent photocatalytic hydrogen evolution rates (up to $5.9 \text{ mmol g}^{-1} \text{ h}^{-1}$). ESR spectroscopic analysis revealed that the photocatalytic reaction proceeded *via* an electron transfer mechanism. We think that the concept of AI-PCA might be applicable to a wide range of photoactive molecules. Further investigations on the effects of organic dyes, morphologies, and the molecular arrangements of supramolecular assemblies on the photocatalytic activity of SA-SPCs, and the detailed mechanism of AI-PCA are currently underway.

Conflicts of interest

There are no conflicts to declare.

Acknowledgements

This work was performed at Osaka University and financially supported by a Grant-in-Aid for Young Scientists (JSPS KAKENHI Grant No. JP18K14189), AMED (Grant No. JP19lm0203007 and JP19lm0203014), Takeda Science Foundation, Kowa Life Science Foundation, Senri Life Science Foundation, and Kato Memorial Bioscience Foundation. We appreciate Mr Y. Murakami for technical support for TEM observation. We also thank Dr Y. Morimoto and Dr K. Oohora for technical support for ESR measurement. We acknowledge Prof. Dr H. Uyama and Dr T. Asoh for DLS measurement.

Notes and references

- 1 C. Xu, P. R. Anusuyadevi, C. Aymonier, R. Luque and S. Marre, *Chem. Soc. Rev.*, 2019, **48**, 3868; J. Li and N. Wu, *Catal. Sci. Technol.*, 2015, **5**, 1360; X. Chen, C. Li, M. Grätzel, R. Kostecki and S. S. Mao, *Chem. Soc. Rev.*, 2012, **41**, 7909; T. Hisatomi, J. Kubota and K. Domen, *Chem. Soc. Rev.*, 2014, **43**, 7520; M. G. Walter, E. L. Warren, J. R. McKone, S. W. Boettcher, Q. Mi, E. A. Santori and N. S. Lewis, *Chem. Rev.*, 2010, **110**, 6446.
- 2 A. Fujishima and K. Honda, *Nature*, 1972, **238**, 37; K. Hashimoto, H. Irie and A. Fujishima, *Jpn. J. Appl. Phys.*, 2005, **44**, 8269.
- 3 J. Xing, W. Q. Fang, H. J. Zhao and H. G. Yang, *Chem.-Asian J.*, 2012, **7**, 642; S. Dong, J. Feng, M. Fan, Y. Pi, L. Hu, X. Han, M. Liu, J. Sun and J. Sun, *RSC Adv.*, 2015, **5**, 14610; M. A. Fox and M. T. Dulay, *Chem. Rev.*, 1993, **93**, 341; Q. Tian, W. Yao, W. Wu and C. Jiang, *Nanoscale Horiz.*, 2019, **4**, 10; L. Wnag, X. Xu, Q. Cheng, S. X. Dou and Y. Du, *Small*, 2019, 1904107.
- 4 *Visible light photocatalysis in organic chemistry*, ed. C. R. J. Stephenson, T. P. Yoon and D. W. C. MacMillan, Wiley-VCH, 2018; A. J. Esswein and D. G. Nocera, *Chem. Rev.*, 2007, **107**, 4022; I. Ghosh, J. Khamrai, A. Savateev, N. Shlapakov, M. Antonietti and B. König, *Science*, 2019, **365**, 360; M. Giedyk, R. Narobe, S. Weiß, D. Touraud, W. Kunz and B. König, *Nat. Catal.*, 2020, **3**, 40.

- 5 X. Wang, K. Maeda, A. Thomas, K. Takanabe, G. Xin, J. M. Carlsson, K. Domen and M. Antonietti, *Nat. Mater.*, 2009, **8**, 76; R. S. Sprick, J. Jiang, B. Bonillo, S. Ren, T. Ratvijitvech, P. Guiglion, M. A. Zwijnenburg, D. J. Adams and A. I. Cooper, *J. Am. Chem. Soc.*, 2015, **137**, 3265; M. G. Schwab, M. Hamburger, X. Feng, J. Shu, H. W. Spiess, X. Wang, M. Antonietti and K. Müllen, *Chem. Commun.*, 2010, **46**, 8932; J. Kosco, M. Bidwell, H. Cha, T. Martin, C. T. Howells, M. Sachs, D. H. Anjum, S. G. Lopez, L. Zou, A. Wadsworth, W. Zhang, L. Zhang, J. Tellam, R. Sougrat, F. Laquai, D. M. DeLongchamp, J. R. Durrant and I. McCulloch, *Nat. Mater.*, 2020, **19**, 559; Y. Wang, A. Vogel, M. Sachs, R. S. Sprick, L. Wilbraham, S. J. A. Moniz, R. Godin, M. A. Zwijnenburg, J. R. Durrant, A. I. Cooper and J. Tang, *Nat. Energy*, 2019, **4**, 746; X. Wang, K. Maeda, A. Thomas, K. Takanabe, G. Xin, J. M. Carlsson, K. Domen and M. A. Antonietti, *Nat. Mater.*, 2009, **8**, 76; G. Dong, Y. Zhang, Q. Pan and J. Qiu, *J. Photochem. Photobiol. C*, 2014, **20**, 33; J. Zhang, X. Chen, K. Takanabe, K. Maeda, K. Domen, J. D. Epping, X. Fu, M. Antonietti and X. Wang, *Angew. Chem., Int. Ed.*, 2010, **49**, 441.
- 6 H. Honda, A. Ishizaki, R. Soma, K. Hashimoto and A. Fujishima, *J. Illum. Eng. Soc.*, 1998, **27**, 42; K. Sunada, Y. Kikuchi, K. Hashimoto and A. Fujishima, *Environ. Sci. Technol.*, 1998, **32**, 726; K. Sunada, T. Watanabe and K. Hashimoto, *Environ. Sci. Technol.*, 2003, **37**, 4785.
- 7 C. K. Prier, D. A. Rankic and D. W. MacMillan, *Chem. Rev.*, 2013, **113**, 5322.
- 8 J. Zhao, W. Wu, J. Sun and S. Guo, *Chem. Soc. Rev.*, 2013, **42**, 5323; A. Taniguchi, Y. Shimizu, K. Oisaki, Y. Sohma and M. Kanai, *Nat. Chem.*, 2016, **8**, 974.
- 9 M. S. Kodaimati, K. P. McClelland, C. He, S. Lian, Y. Jiang, Z. Zhang and E. A. Weiss, *Inorg. Chem.*, 2018, **57**, 3659; A. B. Djurišić, Y. He and A. M. C. Ng, *APL Mater.*, 2020, **8**, 030903; Y. Qu and X. Duan, *Chem. Soc. Rev.*, 2013, **42**, 2568; J. K. Stolarczyk, S. Bhattacharyya, L. Polavarapu and J. Feldmann, *ACS Catal.*, 2018, **8**, 3602; P. Moroz, A. Boddy and M. Zamkov, *Front. Chem.*, 2018, **6**, 353.
- 10 Z. Zhao, H. Zhang, J. W. Y. Lam and B. Z. Tang, *Angew. Chem., Int. Ed.*, 2020, **59**, 9888.
- 11 *Photophysics of Aromatic Molecules*, ed. J. B. Birks, John Wiley & Sons Ltd, 1970; M. Shimizu and T. Hiyama, *Chem.-Asian J.*, 2010, **5**, 1516.
- 12 Y. Hong, J. W. Y. Lam and B. Z. Tang, *Chem. Soc. Rev.*, 2011, **40**, 5361; Y. Chen, J. W. Y. Lam, R. T. K. Kwok, B. Liu and B. Z. Tang, *Mater. Horiz.*, 2019, **6**, 428; H. Wang, E. Zhao, J. W. Y. Lam and B. Z. Tang, *Mater. Today*, 2015, **18**, 365.
- 13 D. M. Eisele, C. W. Cone, E. A. Bloemsma, S. M. Vlaming, C. G. F. van der Kwaak, R. J. Silbey, M. G. Bawendi, J. Knoester, J. P. Rabe and D. A. Vanden Bout, *Nat. Chem.*, 2012, **4**, 655; D. M. Eisele, D. H. Arias, X. Fu, E. A. Bloemsma, C. P. Steiner, R. A. Jensen, P. Rebentrost, H. Eisele, A. Tokmakoff, S. Lloyd, K. A. Nelson, D. Nicastro, J. Knoester and M. G. Bawendi, *Proc. Natl. Acad. Sci. U. S. A.*, 2014, **111**, E3367; J.-J. Li, Y. Chen, J. Yu, N. Cheng and Y. A. Liu, *Adv. Mater.*, 2017, **29**, 1701905; K. Trofymchuk,



A. Reisch, P. Didier, F. Fras, P. Gilliot, Y. Mely and A. S. Klymchenko, *Nat. Photonics*, 2017, **11**, 657.

14 N. Yanai and N. Kimizuka, *Chem. Commun.*, 2016, **52**, 5354; P. Duan, N. Yanai, H. Nagatomi and N. Kimizuka, *J. Am. Chem. Soc.*, 2015, **137**, 1887.

15 A. M. Levine, C. Schierl, B. S. Basel, M. Ahmed, B. A. Camargo, D. M. Guldin and A. B. Braunschweig, *J. Phys. Chem. C*, 2019, **123**, 1587; Z. Tang, S. Zhou, X. Wang, H. Liu, X. Yan, S. Liu, X. Lu and X. Li, *J. Mater. Chem. C*, 2019, **7**, 11090.

16 Y. Zeng, J. Chen, T. Yu, G. Yang and Y. Li, *ACS Energy Lett.*, 2017, **2**, 357; M. Hao, G. Sun, M. Zuo, Z. Xu, Y. Chen, X.-Y. Hu and L. Wang, *Angew. Chem., Int. Ed.*, 2020, **59**, 10095.

17 N. Melnychuk and A. S. Klymchenko, *J. Am. Chem. Soc.*, 2018, **140**, 10856; J. Guo, J. Zhuang, F. Wang, K. R. Raghupathi and S. Thayumanavan, *J. Am. Chem. Soc.*, 2014, **136**, 2220.

18 K. Mizusawa, Y. Takaoka and I. Hamachi, *J. Am. Chem. Soc.*, 2012, **134**, 13386; T. Yoshii, K. Mizusawa, Y. Takaoka and I. Hamachi, *J. Am. Chem. Soc.*, 2014, **136**, 16635; T.-C. Hou, Y.-Y. Wu, P.-Y. Chiang and K.-T. Tan, *Chem. Sci.*, 2015, **6**, 4643; Y. Gao, J. Shi, D. Yuan and B. Xu, *Nat. Commun.*, 2012, **3**, 1033; X.-M. Chen, Q. Cao, H. K. Bisoyi, M. Wang, H. Yang and Q. Li, *Angew. Chem., Int. Ed.*, 2020, **59**, 10493.

19 Y. Sasaki, M. Oshikawa, P. Bharmoria, H. Kouno, A. Hayashi-Takagi, M. Sato, I. Ajioka, N. Yanai and N. Kimizuka, *Angew. Chem., Int. Ed.*, 2019, **58**, 17827.

20 X. Li, C.-Y. Kim, S. Lee, D. Lee, H.-M. Chung, G. Kim, S.-H. Heo, C. Kim, K.-S. Hong and J. Yoon, *J. Am. Chem. Soc.*, 2017, **139**, 10880; M. Abbas, Q. Zou, S. Li and X. Yan, *Adv. Mater.*, 2017, **29**, 1605021.

21 R. Zhang, Y. Duan and B. Liu, *Nanoscale*, 2019, **11**, 19241; Z. Liu, H. Zou, Z. Zhao, P. Zhang, G.-G. Shan, R. T. K. Kwok, J. W. Y. Lam, L. Zheng and B. Z. Tang, *ACS Nano*, 2019, **13**, 11283.

22 A. T. Haedler, K. Kreger, A. Issac, B. Wittmann, M. Kivala, N. Hammer, J. Köhler, H.-W. Schmidt and R. Hildner, *Nature*, 2015, **523**, 196; N. Zhang, L. Wang, H. Wang, R. Cao, J. Wang, F. Bai and H. Fan, *Nano Lett.*, 2018, **18**, 560; J. Wang, Y. Zhong, L. Wang, N. Zhang, R. Cao, K. Bian, L. Alarid, R. E. Haddad, F. Bai and H. Fan, *Nano Lett.*, 2016, **16**, 6523; Y. Zhong, J. Wang, R. Zhang, W. Wei, H. Wang, X. Lu, F. Bai, H. Wu, R. Haddad and H. Fan, *Nano Lett.*, 2014, **14**, 7175; Y. Liu, L. Wang, H. Feng, X. Ren, J. Ji, F. Bai and H. Fan, *Nano Lett.*, 2019, **19**, 2614; X. Yang, Z. Hu, Q. Yin, C. Shu, X.-F. Jiang, J. Zhang, X. Wang, J.-X. Jiang, F. Huang and Y. Cao, *Adv. Funct. Mater.*, 2019, **29**, 1808156; A. S. Weingarten, R. V. Kazantsev, L. C. Palmer, M. McClendon, A. R. Koltonow, A. P. S. Samuel, D. J. Kiebala, M. R. Wasielewski and S. I. Stupp, *Nat. Chem.*, 2014, **6**, 964; S. Chen, D. L. Jacobs, J. Xu, Y. Li, C. Wang and L. Zang, *RSC Adv.*, 2014, **4**, 48486; S. Chen, C. Wang, B. R. Bunes, Y. Li, C. Wang and L. Zang, *Appl. Catal., A*, 2015, **498**, 63; D. Liu, J. Wang, X. Bai, R. Zong and Y. Zhu, *Adv. Mater.*, 2016, **28**, 7284; J. Wang, W. Shi, D. Liu, Z. Zhang, Y. Zhu and D. Wang, *Appl. Catal., B*, 2016, **202**, 289; M. C. Nolan, J. J. Walsh, L. L. E. Mears, E. R. Draper, M. Wallace, M. Barrow, B. Dietrich, S. M. King, A. J. Cowan and D. J. Adams, *J. Mater. Chem. A*, 2017, **5**, 7555; J. Yang, H. Miao, W. Li, H. Li and Y. Zhu, *J. Mater. Chem.*, 2019, **7**, 6482; C. L. Smith, L. L. E. Mears, B. J. Greeves, E. R. Draper, J. Doutch, D. J. Adams and A. J. Cowan, *Phys. Chem. Chem. Phys.*, 2019, **21**, 26466; K. Kong, S. Zhang, Y. Chu, Y. Hu, F. Yu, H. Ye, H. Ding and J. Hua, *Chem. Commun.*, 2019, **55**, 8090; J. Wang, D. Liu, Y. Zhu, S. Zhou and S. Guan, *Appl. Catal., B*, 2018, **231**, 251.

23 A. J. Esswein and D. G. Nocera, *Chem. Rev.*, 2007, **107**, 4022; N. A. Romero and D. A. Nicewicz, *Chem. Rev.*, 2016, **116**, 10075.

24 N. J. Hestand, R. V. Kazantsev, A. S. Weingarten, L. C. Palmer, S. I. Stupp and F. C. Spano, *J. Am. Chem. Soc.*, 2016, **138**, 11762.

25 D. B. Amabilino, D. K. Smith and J. W. Steed, *Chem. Soc. Rev.*, 2017, **46**, 2404.

26 T. Aida, E. W. Meijer and S. I. Stupp, *Science*, 2012, **335**, 813.

27 M. Beija, C. A. M. Afonso and J. M. G. Martinho, *Chem. Soc. Rev.*, 2009, **38**, 2410.

28 K. Adachi, K. Watanabe and S. Yamazaki, *Ind. Eng. Chem. Res.*, 2014, **53**, 13046; S. Verma and H. N. Ghosh, *J. Phys. Chem. Lett.*, 2012, **3**, 1877.

29 H. Y. Kim, T. G. Bjorklund, S.-H. Lim and C. J. Bardeen, *Langmuir*, 2003, **19**, 3941.

30 O. Legrini, E. Oliveros and A. M. Braun, *Chem. Rev.*, 1993, **93**, 671; M. R. Hoffman, S. T. Martin, W. Choi and D. W. Bahnemann, *Chem. Rev.*, 1995, **95**, 69; C. Chen, W. Ma and J. Zhao, *Chem. Soc. Rev.*, 2010, **39**, 4206; A. L. Linsebigler, G. Lu and J. T. Yates Jr, *Chem. Rev.*, 1995, **95**, 735.

31 P. Guo, P. Chen, W. Ma and M. J. Liu, *Mater. Chem.*, 2012, **22**, 20243; Y. Yamakoshi, N. Umezawa, A. Ryu, K. Arakane, N. Miyata, Y. Goda, T. Masumizu and T. Nagano, *J. Am. Chem. Soc.*, 2003, **125**, 12803.

32 Y. A. Lion, E. Gandin and A. V. D. Vorst, *Photochem. Photobiol.*, 1980, **31**, 305.

33 P. Xiao, P. Wang, H. Li, Q. Li, Y. Shi, X.-L. Wu, H. Lin, J. Chen and X. Wang, *J. Hazard. Mater.*, 2018, **345**, 123.

34 J. J. M. Lamberts and D. C. Neckers, *Tetrahedron*, 1985, **41**, 2183; M. C. DeRosa and R. J. Crutchley, *Coord. Chem. Rev.*, 2002, **233**–234, 351.

35 V. E. Korobov, V. V. Shubin and A. K. Chibisov, *Chem. Phys. Lett.*, 1977, **45**, 498.

36 *Oxidation-Reduction Potentials of Organic Systems*, ed. W. M. Clark, Williams & Wilkins Co, 1960; A. S. Weingarten, A. J. Dannenhoffer, R. V. Kazantsev, H. Sai, D. Huang and S. I. Stupp, *J. Am. Chem. Soc.*, 2018, **140**, 4965.

37 S. Guo, Z. Deng, M. Li, B. Jiang, C. Tian, Q. Pan and H. Fu, *Angew. Chem., Int. Ed.*, 2016, **55**, 1830.

38 X. Wang, L. Chen, S. Y. Chong, M. A. Little, Y. Wu, W.-H. Zhu, R. Clowes, Y. Yan, M. A. Zwijnenburg, R. S. Sprick and A. I. Cooper, *Nat. Chem.*, 2018, **10**, 1180.

39 M. F. Mark, M. W. Kryman, M. R. Detty and D. W. McCamant, *J. Phys. Chem. C*, 2018, **122**, 16519.

